BONN-TH-2005-04
WUE-ITP-2005-010
hep-ph/0508267

arXiv:hep-ph/0508267v2 4 Nov 2005

Higgs boson interference in $\mu^+\mu^- \to \tilde{\chi}_i^+\tilde{\chi}_j^-$ with longitudinally polarized beams

Olaf Kittel[a], Federico von der Pahlen[b]

[a] *Physikalisches Institut der Universität Bonn,*
Nussallee 12, D-53115 Bonn, Germany

[b] *Institut für Theoretische Physik und Astrophysik, Universität Würzburg,*
Am Hubland, D-97074 Würzburg, Germany

Abstract

We study chargino production at a muon collider with longitudinally polarized beams and center of mass energies around the heavy neutral Higgs boson resonances. We show that the interference of the CP even and CP odd Higgs bosons can be analyzed using the energy distributions of the lepton or W boson from the chargino two-body decays $\tilde{\chi}_j^\pm \to \ell^\pm \tilde{\nu}_\ell$ or $\tilde{\chi}_j^\pm \to W^\pm \tilde{\chi}_1^0$, respectively. The energy distributions depend on the longitudinal polarization of the decaying chargino, which are correlated to the muon beam polarizations. We define asymmetries in these energy distributions which allow a determination of the H and A couplings to the charginos and in particular of their relative phase. We analyze the asymmetries, cross sections and branching ratios in CP conserving Minimal Supersymmetric Standard Model scenarios. For nearly degenerate Higgs bosons we find maximal asymmetries which can be measured with high statistical significance.

1 Introduction

The CP conserving Minimal Supersymmetric Standard Model (MSSM) contains three neutral Higgs bosons, a light scalar h, a heavier scalar H, and a pseudoscalar A [1, 2, 3]. A muon collider is an excellent tool to study the properties of these neutral Higgs bosons, since they are resonantly produced in s-channels [3, 4, 5, 6]. A scan of the production line shape around the resonance region allows the determination of e.g. the H and A masses and widths, if the overlap of the two resonances is not too large [6]. Moreover, if the polarizations of the muon beams *and* the final particles are taken into account, interference effects of the H and A channels give valuable information on the CP properties of the Higgs bosons [7]. The H–A interference has been studied recently in [8], where the interactions of the Higgs bosons with neutralinos, the supersymmetric partners of the neutral Higgs and gauge bosons, have been analyzed.

In this paper we study the production of charginos, the supersymmetric partners of the charged Higgs and gauge bosons, which allows precision measurements of the Higgs-chargino couplings [9]. We show that the longitudinal chargino polarizations are sensitive to the interference of the H and A channels, which is sizable if the two Higgs bosons are nearly degenerate, i.e. if their mass difference is of the order of their decay widths. In order to probe the longitudinal chargino polarizations, we define asymmetries in the energy distribution of the lepton ℓ from the chargino decay $\tilde{\chi}_j^\pm \to \ell^\pm \tilde{\nu}_\ell^{(*)}$, and the W boson from the chargino decay $\tilde{\chi}_j^\pm \to W^\pm \tilde{\chi}_k^0$. A measurement of these asymmetries and the cross sections allows a determination of the Higgs-chargino couplings. In particular the asymmetries provide the relative phase between the CP even and CP odd Higgs boson couplings, which would be a unique test of their CP properties.

In Section 2 we give our definitions and formalism, and define the energy distribution asymmetries. In Section 3 we study the dependence of these asymmetries on the Higgs-chargino couplings. In Section 4 we present numerical results and give a summary and conclusions in Section 5.

2 Definitions and formalism

We study pair production of charginos with momentum p and helicity λ

$$\mu^+ + \mu^- \to \tilde{\chi}_i^\mp(p_{\chi_i^\mp}, \lambda_i) + \tilde{\chi}_j^\pm(p_{\chi_j^\pm}, \lambda_j) \tag{1}$$

with longitudinally polarized muon beams, and the subsequent leptonic two-body decay of one of the charginos into a lepton and a sneutrino

$$\tilde{\chi}_j^\pm \to \ell^\pm + \tilde{\nu}_\ell^{(*)}. \tag{2}$$

In the following we focus on the case $\ell = e, \mu$. However, the results we obtain can be extended for $\ell = \tau$ and for the chargino decay into a W boson and a neutralino,

$$\tilde{\chi}_j^\pm \to W^\pm + \tilde{\chi}_k^0, \tag{3}$$

for which we give relevant formulas in Appendix B.

2.1 Lagrangians and couplings

The MSSM interaction Lagrangians for chargino production (1) via Higgs exchange are (in our notation we follow closely [1, 2, 8])

$$\mathcal{L}_{\mu^+\mu^-\phi} = g\,\bar{\mu}\,(c^{(\phi\mu)\,*}P_L + c^{(\phi\mu)}P_R)\,\mu\,\phi, \tag{4}$$

$$\mathcal{L}_{\tilde{\chi}^+\tilde{\chi}^+\phi} = g\,\bar{\tilde{\chi}}_i^+(c_{L\,ij}^{(\phi)}P_L + c_{R\,ij}^{(\phi)}P_R)\tilde{\chi}_j^+\,\phi, \tag{5}$$

with $P_{R,L} = \frac{1}{2}(1 \pm \gamma^5)$, g the weak coupling constant and $\phi = H, A, h$. The muon and chargino couplings to H and A are [2]:

$$c^{(H\mu)} = -\frac{m_\mu}{2m_W}\frac{\cos\alpha}{\cos\beta}, \tag{6}$$

$$c^{(A\mu)} = i\frac{m_\mu}{2m_W}\tan\beta, \tag{7}$$

$$c_{L\,ij}^{(H)} = -Q_{ij}^*\cos\alpha - S_{ij}^*\sin\alpha, \tag{8}$$

$$c_{L\,ij}^{(A)} = i(Q_{ij}^*\sin\beta + S_{ij}^*\cos\beta), \tag{9}$$

$$c_{R\,ij}^{(\phi)} = c_{L\,ji}^{(\phi)*}, \quad \phi = H, A, \tag{10}$$

$$Q_{ij} = \frac{1}{\sqrt{2}}U_{i2}V_{j1}, \tag{11}$$

$$S_{ij} = \frac{1}{\sqrt{2}}U_{i1}V_{j2}, \tag{12}$$

where α is the Higgs mixing angle, $\tan\beta = v_2/v_1$ is the ratio of the vacuum expectation values of the two neutral Higgs fields, θ_W is the weak mixing angle and U, V are the 2×2 matrices which diagonalize the chargino mass matrix X with $U_{m\alpha}^*\,X_{\alpha\beta}\,V_{\beta n}^{-1} = m_{\chi_m^\pm}\,\delta_{mn}$ [1]. The muon and chargino couplings to the lighter Higgs boson h are obtained by substituting α with $\alpha + \pi/2$ in (6) and (8).

The Lagrangian for chargino decay into a lepton and a sneutrino (2) is

$$\mathcal{L}_{\ell\tilde{\nu}_\ell\tilde{\chi}^+} = -gV_{j1}\bar{\ell}P_R\tilde{\chi}_j^{+C}\tilde{\nu}_\ell + \text{h.c.}, \qquad \ell = e, \mu. \tag{13}$$

The Lagrangians for $\ell = \tau$ and for the chargino decay into a W boson and a neutralino (3) are given in Appendix B.

2.2 Amplitudes and spin density matrix formalism

For the calculation of the cross section for the combined process of chargino production (1) and decay, (2) or (3), which includes the chargino $\tilde{\chi}_j^\pm$ helicities λ_j, we use the spin density matrix formalism of [10], as e.g. used for chargino production in e^+e^- annihilation in [11]. The unnormalized spin density matrices ρ^P of $\tilde{\chi}_i^\mp\tilde{\chi}_j^\pm$ production and ρ^D of $\tilde{\chi}_j^\pm$ decay are given by

$$\rho^P_{\lambda_j\lambda_j'} = \sum_{\lambda_i} T^P_{\lambda_i\lambda_j}T^{P*}_{\lambda_i\lambda_j'}, \tag{14}$$

$$\rho^D_{\lambda_j'\lambda_j} = T^{D*}_{\lambda_j'}T^D_{\lambda_j}, \tag{15}$$

where $T^P_{\lambda_i\lambda_j}$ and $T^D_{\lambda_j}$ are the helicity amplitudes for production and decay, respectively. The amplitude squared for production and decay is then

$$|T|^2 = |\Delta(\tilde{\chi}^\pm_j)|^2 \sum_{\lambda_j\lambda'_j} \rho^P_{\lambda_j\lambda'_j}\rho^D_{\lambda'_j\lambda_j}, \tag{16}$$

with the propagator $\Delta(\tilde{\chi}^\pm_j) = i/[p^2_{\chi^\pm_j} - m^2_{\chi^\pm_j} + im_{\chi^\pm_j}\Gamma_{\chi^\pm_j}]$, where $p_{\chi^\pm_j}$, $m_{\chi^\pm_j}$ and $\Gamma_{\chi^\pm_j}$ denote the four-momentum, mass and width of the chargino, respectively.

Introducing a set of chargino spin vectors $s^a_{\chi^\pm_j}$, given in Appendix A, the spin density matrices (14) and (15) can be expanded in terms of the Pauli matrices τ^a

$$\rho^P_{\lambda_j\lambda'_j} = \delta_{\lambda_j\lambda'_j} P + \sum_{a=1}^{3} \tau^a_{\lambda_j\lambda'_j}\Sigma^a_P, \tag{17}$$

$$\rho^D_{\lambda'_j\lambda_j} = \delta_{\lambda'_j\lambda_j} D + \sum_{a=1}^{3} \tau^a_{\lambda'_j\lambda_j}\Sigma^a_D. \tag{18}$$

With our choice of the spin vectors, Σ^3_P/P is the longitudinal polarization of $\tilde{\chi}^\pm_j$, Σ^1_P/P is the transverse polarization in the production plane and Σ^2_P/P is the polarization perpendicular to the production plane. Inserting the density matrices (17) and (18) into (16) gives

$$|T|^2 = 2|\Delta(\tilde{\chi}^\pm_j)|^2 (PD + \sum_{a=1}^{3} \Sigma^a_P\Sigma^a_D). \tag{19}$$

The first term in (19) is independent of the chargino polarization whereas the second term describes the spin correlations between production and decay. Cross sections and distributions are now obtained by integrating $|T|^2$ over the Lorentz invariant phase space element dLips

$$d\sigma = \frac{1}{2s}|T|^2 d\text{Lips}, \tag{20}$$

where we use the narrow width approximation for the propagator of the decaying chargino. Explicit formulas of the phase space for chargino production (1) and decay, (2) or (3), can be found e.g. in [12].

2.2.1 Contributions from H and A exchange

The expansion coefficients of the chargino production matrix (17) subdivide into contributions from the Higgs resonances and the continuum, respectively,

$$P = P_r + P_{cont}, \qquad \Sigma^a_P = \Sigma^a_r + \Sigma^a_{cont} \; . \tag{21}$$

The continuum contributions P_{cont}, Σ^a_{cont} are those from the non-resonant γ, Z and $\tilde{\nu}_\mu$ exchange channels and can be found in [11]. The resonant contributions are those from s-channel exchange of the Higgs bosons H and A

$$P_r = \sum_{\phi=H,A} P_r^{(\phi\phi)} + P_r^{(HA)}, \tag{22}$$

$$\Sigma^3_r = \sum_{\phi=H,A} \Sigma_r^{3\,(\phi\phi)} + \Sigma_r^{3\,(HA)}, \tag{23}$$

which read for $\mu^+\mu^- \to \tilde{\chi}_i^- \tilde{\chi}_j^+$

$$\begin{aligned} P_r^{(\phi\phi)} &= \frac{g^4}{4}(1+\mathcal{P}_+\mathcal{P}_-)|\Delta(\phi)|^2 |c^{(\phi\mu)}|^2 \\ &\quad \Big[(|c_L^{(\phi)}|^2 + |c_R^{(\phi)}|^2)(s - m^2_{\chi_i^\pm} - m^2_{\chi_j^\pm}) - 4\mathrm{Re}\{c_L^{(\phi)} c_R^{(\phi)\,*}\} m_{\chi_i^\pm} m_{\chi_j^\pm}\Big]\, s, \end{aligned} \tag{24}$$

$$\begin{aligned} P_r^{(HA)} &= -\frac{g^4}{2}(\mathcal{P}_+ + \mathcal{P}_-)\mathrm{Re}\{\Delta(H)\Delta(A)^*\}\mathrm{Im}\{c^{(H\mu)} c^{(A\mu)^*}\} \\ &\quad \Big[\mathrm{Im}\{c_L^{(H)} c_L^{(A)\,*} + c_R^{(H)} c_R^{(A)\,*}\}(s - m^2_{\chi_i^\pm} - m^2_{\chi_j^\pm}) \\ &\quad -2\,\mathrm{Im}\{c_L^{(H)} c_R^{(A)\,*} + c_R^{(H)} c_L^{(A)\,*}\} m_{\chi_i^\pm} m_{\chi_j^\pm}\Big]\, s, \end{aligned} \tag{25}$$

$$\Sigma_r^{3\,(\phi\phi)} = \frac{g^4}{4}(1+\mathcal{P}_+\mathcal{P}_-)|\Delta(\phi)|^2 |c^{(\phi\mu)}|^2 (|c_L^{(\phi)}|^2 - |c_R^{(\phi)}|^2) s\sqrt{\lambda_{ij}}, \tag{26}$$

$$\begin{aligned} \Sigma_r^{3\,(HA)} &= -\frac{g^4}{2}\mathrm{Re}\{\Delta(H)\Delta(A)^*\}(\mathcal{P}_+ + \mathcal{P}_-) \\ &\quad \mathrm{Im}\{c_L^{(H)} c_L^{(A)*} - c_R^{(H)} c_R^{(A)*}\}\mathrm{Im}\{c^{(H\mu)} c^{(A\mu)*}\} s\sqrt{\lambda_{ij}}. \end{aligned} \tag{27}$$

The resonant contributions Σ_r^1 and Σ_r^2 to the transverse polarizations of the chargino vanish, since the s-channel exchange is due to scalar Higgs bosons. In the above formulas the chargino indices of the couplings $c_R^{(\phi)} \equiv c_{R\,ij}^{(\phi)}$ and $c_L^{(\phi)} \equiv c_{L\,ij}^{(\phi)}$ have been suppressed, the longitudinal beam polarizations are denoted by $\mathcal{P}_+$, $\mathcal{P}_-$, and

$$\Delta(\phi) = i[(s - m_\phi^2) + i m_\phi \Gamma_\phi]^{-1}, \qquad \phi = H, A, \tag{28}$$

$$\lambda_{ij} = \lambda(s, m^2_{\chi_i^\pm}, m^2_{\chi_j^\pm}), \tag{29}$$

with $\lambda(x,y,z) = x^2+y^2+z^2-2(xy+xz+yz)$. Note that both $P_r^{(HA)}$ and $\Sigma_r^{3\,(\phi\phi)}$ vanish for production of equal charginos $i = j$ since then the Higgs-chargino couplings are parity conserving, with $c_{L\,ii}^{(\phi)} = c_{R\,ii}^{(\phi)*}$. These two terms are only present for $\tilde{\chi}_1^\pm \tilde{\chi}_2^\mp$ production since $c_{L\,ij}^{(\phi)} \neq c_{R\,ij}^{(\phi)*}$ for $i \neq j$ in general. We neglect interferences of the chirality violating Higgs exchange amplitudes with the chirality conserving continuum amplitudes, which are of order $m_\mu/\sqrt{s}$. Further we neglect contributions from h exchange far from its resonance.

In order to find observables which are sensitive to the H–A interference, we analyze the properties of the coefficients P and Σ_P^3 (21) under parity and charge conjugation. For the production of the charge conjugated pair of charginos $\mu^+\mu^- \to \tilde{\chi}_i^+ \tilde{\chi}_j^-$ they transform into

$$\Sigma^3_{cont} \to -\Sigma^3_{cont}, \tag{30}$$

$$P_r^{(HA)} \to -P_r^{(HA)}, \tag{31}$$

$$\Sigma_r^{3\,(\phi\phi)} \to -\Sigma_r^{3\,(\phi\phi)}, \tag{32}$$

while P_{cont} [11], $P_r^{(\phi\phi)}$ and $\Sigma_r^{3\,(HA)}$ do not change. For equal beam polarizations $\mathcal{P}_+ = \mathcal{P}_- \equiv \mathcal{P}$ the resonant contributions transform under $\mathcal{P} \to -\mathcal{P}$ into

$$P_r^{(HA)} \to -P_r^{(HA)}, \tag{33}$$

$$\Sigma_r^{3\,(HA)} \to -\Sigma_r^{3\,(HA)}, \tag{34}$$

while the terms $P_r^{(\phi\phi)}$, $\Sigma_r^{3\,(\phi\phi)}$ and the continuum contributions P_{cont} and Σ^3_{cont} [11], are invariant. Note that the H–A interference terms $P_r^{(HA)}$ (25) and $\Sigma_r^{3\,(HA)}$ (27) are parity odd and thus vanish for zero beam polarizations $\mathcal{P}_+ = \mathcal{P}_- = 0$.

2.2.2 Chargino decay into electrons and muons

The expansion coefficients of the chargino decay matrix (18) for the chargino decay $\tilde{\chi}_j^+ \to \ell^+ \, \tilde{\nu}_\ell$, with $\ell = e, \mu$, are

$$\begin{aligned} D &= \frac{g^2}{2}|V_{j1}|^2(m^2_{\chi_j^\pm} - m^2_{\tilde{\nu}_\ell}), && (35)\\ \Sigma_D^a &= -g^2|V_{j1}|^2 m_{\chi_j^\pm}(s^a_{\chi_j^\pm}\cdot p_\ell). && (36) \end{aligned}$$

The coefficient Σ_D^a for the charge conjugated process, $\tilde{\chi}_j^- \to \ell^- \, \tilde{\nu}_\ell^*$, is obtained by inverting the sign of (36). The coefficients for $\ell = \tau$ and for chargino decay into a W boson and a neutralino are given in Appendix B.

2.3 Energy distribution

In the center of mass system (CMS), the kinematical limits of the energy of the decay particle $\lambda = e, \mu, \tau, W$ from the chargino decays (2) and (3) are

$$E_\lambda^{max(min)} = \bar{E}_\lambda \pm \Delta_\lambda, \qquad (37)$$

which read for the leptonic ($\lambda = \ell$) chargino decays

$$\begin{aligned} \bar{E}_\ell &= \frac{E_\ell^{max} + E_\ell^{min}}{2} = \frac{m^2_{\chi_j^\pm} - m^2_{\tilde{\nu}_\ell}}{2m^2_{\chi_j^\pm}} E_{\chi_j^\pm}, && (38)\\ \Delta_\ell &= \frac{E_\ell^{max} - E_\ell^{min}}{2} = \frac{m^2_{\chi_j^\pm} - m^2_{\tilde{\nu}_\ell}}{2m^2_{\chi_j^\pm}} |\vec{p}_{\chi_j^\pm}|, \qquad \ell = e, \mu, \tau. && (39) \end{aligned}$$

With these definitions we can rewrite the factor Σ_D^3 (36), that multiplies the longitudinal chargino polarization Σ_P^3 in (19),

$$\Sigma_D^3 = \eta_{\lambda^\pm}\frac{D}{\Delta_\lambda}(E_\lambda - \bar{E}_\lambda), \quad \lambda = e, \mu, \tau, W, \qquad (40)$$

where we have used

$$m_{\chi_j^\pm}(s^3_{\chi_j^\pm}\cdot p_\lambda) = -\frac{m^2_{\chi_j^\pm}}{|\vec{p}_{\chi_j^\pm}|}(E_\lambda - \bar{E}_\lambda). \qquad (41)$$

The factor $\eta_{\lambda^\pm}$ is a measure of parity violation, which is maximal $\eta_{\ell^\pm} = \pm 1$ for the decay $\tilde{\chi}_j^\pm \to \ell^\pm \, \tilde{\nu}_\ell^{(*)}$, for $\ell = e, \mu$, since the sneutrino couples purely left handed. For $\ell = \tau$ or for chargino decays into a W and a neutralino, the factors $\eta_{\tau^\pm}$ (B.14) and $\eta_{W^\pm}$ (B.15), respectively, are generally smaller, thus reducing Σ_D^3.

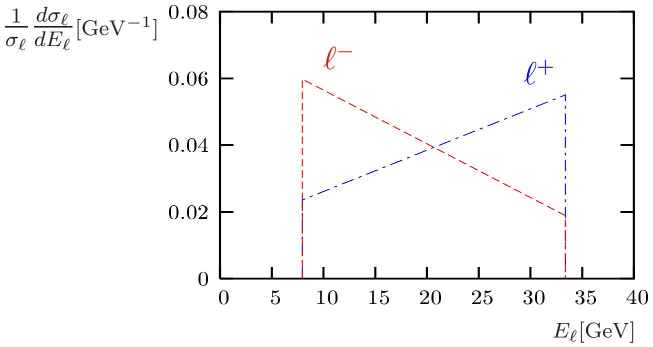

Figure 1: Normalized energy distributions of the lepton for the process $\mu^+\mu^- \to \tilde{\chi}_1^+\tilde{\chi}_1^-$ and decay $\tilde{\chi}_1^+ \to \ell^+\tilde{\nu}_\ell$ (dot-dashed) or $\tilde{\chi}_1^- \to \ell^-\tilde{\nu}_\ell^*$ (dashed), for $\ell = e, \mu$, with $\sqrt{s} = 500$ GeV and longitudinal beam polarizations $\mathcal{P}_+ = \mathcal{P}_- = -0.3$. The MSSM parameters are given in Table 1. The shown distributions have asymmetries $\mathcal{A}_{\ell^+} = 0.2$ and $\mathcal{A}_{\ell^-} = -0.26$, see (44).

The energy distribution of the decay particle $\lambda^\pm$ is now given by

$$\frac{d\sigma_{\lambda^\pm}}{dE_\lambda} = \frac{\sigma_\lambda}{2\Delta_\lambda}\left[1 + \eta_{\lambda^\pm}\frac{\bar{\Sigma}_P^3}{\bar{P}}\frac{(E_\lambda - \bar{E}_\lambda)}{\Delta_\lambda}\right], \tag{42}$$

where we have defined averages over the chargino production angles in the CMS by

$$\bar{P} = \frac{1}{4\pi}\int P d\Omega_{\chi^\pm}, \qquad \bar{\Sigma}_P^3 = \frac{1}{4\pi}\int \Sigma_P^3 d\Omega_{\chi^\pm}. \tag{43}$$

Two examples of energy distributions of the decay particles ℓ^+ and ℓ^-, for $\ell = e, \mu$, are shown in Fig. 1. One can see the linear dependence of the distributions on the lepton energy. The slope of the curves is proportional to the longitudinal chargino polarization. Note that the energy distribution might be difficult to measure for a small chargino-sneutrino mass difference, since the energy span of the observed lepton is proportional to the difference of their squared masses, see (39).

2.4 Asymmetries of the energy distribution

For the cross section $\sigma_{\lambda^\pm}$ of chargino production (1) with subsequent two body decay of one chargino into a lepton and a sneutrino (2) or into a W boson and a neutralino (3), we define the asymmetries $\mathcal{A}_{\lambda^+}$ and $\mathcal{A}_{\lambda^-}$ for the charge conjugated processes

$$\mathcal{A}_{\lambda^\pm} = \frac{\sigma_{\lambda^\pm}(E_\lambda > \bar{E}_\lambda) - \sigma_{\lambda^\pm}(E_\lambda < \bar{E}_\lambda)}{\sigma_{\lambda^\pm}(E_\lambda > \bar{E}_\lambda) + \sigma_{\lambda^\pm}(E_\lambda < \bar{E}_\lambda)}, \qquad \lambda = e, \mu, \tau, W. \tag{44}$$

Using the formula for the energy distribution of the decay particle $\lambda^\pm$ (42), we find that the asymmetries are proportional to the averaged longitudinal chargino polarization

$$\mathcal{A}_{\lambda^\pm} = \frac{1}{2}\eta_{\lambda^\pm}\frac{\bar{\Sigma}_P^3}{\bar{P}}. \tag{45}$$

In order to separate the resonant contributions of the Higgs exchange channels to $\bar{\Sigma}^3_P$ from those of the continuum contributions, see (21) and (43), we use their different dependence on the chargino charge and on the beam polarizations. Therefore it is useful to discuss the production of equal and unequal charginos separately.

2.4.1 Production of equal charginos

If equal charginos are produced, $\mu^+\mu^- \to \tilde{\chi}^+_j \tilde{\chi}^-_j$, the resonant contributions $\Sigma^{3\,(HA)}_r$ are independent of the chargino charge. The continuum contributions Σ^3_{cont}, however, differ by a sign for charginos with positive or negative charge, see (30), and are thus eliminated in the numerator of the charge asymmetries

$$\begin{aligned} \mathcal{A}^C_\lambda &= \frac{1}{2}[\mathcal{A}_{\lambda^+} - \mathcal{A}_{\lambda^-}] && (46) \\ &= \frac{1}{2}\eta_{\lambda^+}\frac{\Sigma^{3\,(HA)}_r}{\bar{P}}, \qquad \lambda = e, \mu, \tau, W, && (47) \end{aligned}$$

with $\bar{\Sigma}^{3\,(HA)}_r = \Sigma^{3\,(HA)}_r$, see (43). The resonant contributions can also be isolated from the continuum contributions by taking into account their different dependence on the beam polarizations for $\mathcal{P} \equiv \mathcal{P}_+ = \mathcal{P}_-$, given in (33), (34). Then the invariant continuum contributions are eliminated in the polarization asymmetries

$$\begin{aligned} \mathcal{A}^{pol}_{\lambda^\pm} &= \frac{1}{2}[\mathcal{A}_{\lambda^\pm}(\mathcal{P}) - \mathcal{A}_{\lambda^\pm}(-\mathcal{P})] && (48) \\ &= \frac{1}{2}\eta_{\lambda^\pm}\frac{\Sigma^{3\,(HA)}_r(\mathcal{P})}{\bar{P}}. && (49) \end{aligned}$$

Since $\Sigma^{3\,(HA)}_r$ (27) describes the interference of the H and A exchange amplitudes, nonvanishing asymmetries $\mathcal{A}^C_\lambda$ and $\mathcal{A}^{pol}_{\lambda^\pm}$ are a clear indication of nearly degenerate scalar resonances with opposite CP quantum numbers in the production of equal charginos.

2.4.2 Production of $\tilde{\chi}^\pm_1 \tilde{\chi}^\mp_2$

The asymmetries $\mathcal{A}^C_\lambda$ (47) and $\mathcal{A}^{pol}_{\lambda^\pm}$ (49) have to be generalized for the production of unequal charginos, $\tilde{\chi}^\mp_1 \tilde{\chi}^\pm_2$, since the coefficient $P^{(HA)}_r$ (25) does not vanish. For either the decay of $\tilde{\chi}^\pm_1$ or the decay of $\tilde{\chi}^\pm_2$ we define the generalized charge asymmetry

$$\tilde{\mathcal{A}}^C_\lambda = \frac{\sigma^>_{\lambda^+} - \sigma^<_{\lambda^+} - \sigma^>_{\lambda^-} + \sigma^<_{\lambda^-}}{\sigma^>_{\lambda^+} + \sigma^<_{\lambda^+} + \sigma^>_{\lambda^-} + \sigma^<_{\lambda^-}}, \qquad \lambda = e, \mu, \tau, W, \tag{50}$$

with the short hand notation $\sigma^>_{\lambda^\pm} = \sigma_{\lambda^\pm}(E_\lambda > \bar{E}_\lambda)$ and $\sigma^<_{\lambda^\pm} = \sigma_{\lambda^\pm}(E_\lambda < \bar{E}_\lambda)$. Using the definition of the energy distribution (42) and the chargino charge transformation properties of the coefficients P and Σ^3_P, (30)-(32), the resonant contributions can be separated, in analogy to (47),

$$\tilde{\mathcal{A}}^C_\lambda = \frac{1}{2}\eta_{\lambda^+}\frac{\Sigma^{3\,(HA)}_r}{\bar{P}_{cont} + P^{(HH)}_r + P^{(AA)}_r}, \tag{51}$$

with $\bar{P}_r^{(\phi\phi)} = P_r^{(\phi\phi)}$. Analogously we define the generalized polarization asymmetry

$$\begin{aligned}
\tilde{\mathcal{A}}_{\lambda^\pm}^{pol} &= \frac{\sigma_{\lambda^\pm}^{>}(\mathcal{P}) - \sigma_{\lambda^\pm}^{<}(\mathcal{P}) - \sigma_{\lambda^\pm}^{>}(-\mathcal{P}) + \sigma_{\lambda^\pm}^{<}(-\mathcal{P})}{\sigma_{\lambda^\pm}^{>}(\mathcal{P}) + \sigma_{\lambda^\pm}^{<}(\mathcal{P}) + \sigma_{\lambda^\pm}^{>}(-\mathcal{P}) + \sigma_{\lambda^\pm}^{<}(-\mathcal{P})} && (52)\\
&= \frac{1}{2}\eta_{\lambda^\pm} \frac{\Sigma_r^{3\,(HA)}(\mathcal{P})}{\bar{P}_{cont} + P_r^{(HH)} + P_r^{(AA)}}, \qquad \lambda = e, \mu, \tau, W, && (53)
\end{aligned}$$

for equal beam polarizations $\mathcal{P}$. For the production of equal charginos these asymmetries reduce to their equivalents $\mathcal{A}_\lambda^C$ and $\mathcal{A}_{\lambda^\pm}^{pol}$, defined in (47) and (49), respectively.

Moreover we define the production asymmetry of the chargino cross sections

$$\mathcal{A}_{prod}^C = \frac{\sigma(\tilde{\chi}_1^+\tilde{\chi}_2^-) - \sigma(\tilde{\chi}_2^+\tilde{\chi}_1^-)}{\sigma(\tilde{\chi}_1^+\tilde{\chi}_2^-) + \sigma(\tilde{\chi}_2^+\tilde{\chi}_1^-)} = \frac{P_r^{(HA)}}{\bar{P}_{cont} + P_r^{(HH)} + P_r^{(AA)}}, \tag{54}$$

which is sensitive to the interference of the H and A channels due to the parity violating Higgs-chargino couplings.

2.4.3 Statistical significances

We define the statistical significance of the asymmetries $\mathcal{A}_{\lambda^\pm}$ by

$$\mathcal{S}_{\lambda^\pm} \;=\; |\mathcal{A}_{\lambda^\pm}|\sqrt{\sigma(\mu^+\mu^- \to \tilde{\chi}_i^\mp\tilde{\chi}_j^\pm)\mathrm{BR}(\tilde{\chi}_j^\pm \to \lambda^\pm\tilde{N}_\lambda)\mathcal{L}_{eff}}, \tag{55}$$

with $\lambda = \ell$ or W and $\tilde{N}_\lambda$ the associated sneutrino or neutralino, respectively. Further the effective integrated luminosity $\mathcal{L}_{eff} = \epsilon_\lambda\mathcal{L}$ depends on the detection efficiency ϵ_λ of leptons or W bosons in the processes $\tilde{\chi}_j^\pm \to \ell^\pm\, \tilde{\nu}_\ell^{(*)}$ or $\tilde{\chi}_j^\pm \to W^\pm\, \tilde{\chi}_k^0$, respectively. The statistical significance for the charge asymmetry $\mathcal{A}_\lambda^C$ is given by

$$\mathcal{S}_\lambda^C \;=\; |\mathcal{A}_\lambda^C|\sqrt{2\,\sigma(\mu^+\mu^- \to \tilde{\chi}_i^-\tilde{\chi}_j^+)\mathrm{BR}(\tilde{\chi}_j^+ \to \lambda^+\tilde{N}_\lambda)\mathcal{L}_{eff}}, \tag{56}$$

which follows from (46). Assuming that $\mathcal{A}_{\lambda^\pm}(\mathcal{P})$ and $\mathcal{A}_{\lambda^\pm}(-\mathcal{P})$ are both obtained with the same integrated luminosity $\mathcal{L}$, we define the statistical significance for the polarization asymmetry $\mathcal{A}_{\lambda^\pm}^{pol}$ by

$$\mathcal{S}_{\lambda^\pm}^{pol} \;=\; |\mathcal{A}_{\lambda^\pm}^{pol}|\sqrt{2\,\sigma(\mu^+\mu^- \to \tilde{\chi}_i^\mp\tilde{\chi}_j^\pm)\mathrm{BR}(\tilde{\chi}_j^\pm \to \lambda^\pm\tilde{N}_\lambda)\mathcal{L}_{eff}}, \tag{57}$$

which follows from (48). For the production asymmetry $\mathcal{A}_{prod}^C$ (54) we define the significance

$$\mathcal{S}_{prod}^C \;=\; |\mathcal{A}_{prod}^C|\sqrt{[\sigma(\tilde{\chi}_1^+\tilde{\chi}_2^-) + \sigma(\tilde{\chi}_2^+\tilde{\chi}_1^-)]\mathcal{L}_{eff}^{prod}}, \tag{58}$$

with $\mathcal{L}_{eff}^{prod}$ the effective integrated luminosity for chargino production.

3 Determination of the Higgs-chargino couplings

In the previous section we have shown that the coefficient Σ_r^3 (27) of the longitudinal chargino polarization is sensitive to the interference of the H and A Higgs bosons. Their interference determines the sign γ of the product of couplings

$$\kappa = \mathrm{Im}\{c^{(H\mu)}c^{(A\mu)*}\}\mathrm{Im}\{c_R^{(H)}c_R^{(A)*}\} = \gamma\, |c^{(H\mu)}c^{(A\mu)}c_R^{(H)}c_R^{(A)}|, \tag{59}$$

which appears in

$$\Sigma_r^{3(HA)} = 2g^4\mathcal{P}\mathrm{Re}\{\Delta(H)\Delta(A)^*\}\mathrm{Im}\{c^{(H\mu)}c^{(A\mu)*}\}\mathrm{Im}\{c_R^{(H)}c_R^{(A)*}\}s\sqrt{\lambda_{11}}, \tag{60}$$

where we focus on the production of the lightest pair of charginos $\mu^+\mu^- \to \tilde{\chi}_1^+\tilde{\chi}_1^-$ with equal muon beam polarizations $\mathcal{P}_+ = \mathcal{P}_- \equiv \mathcal{P}$. Since we assume CP conservation, γ can take the value ±1 for interfering amplitudes of opposite CP eigenvalues, and vanishes for interfering amplitudes with same CP eigenvalues. A measurement of γ would thus be a unique test of the CP properties of the Higgs sector in the underlying supersymmetric model.

The coefficient $\Sigma_r^{3(HA)}$ can be obtained from the chargino production cross section

$$\sigma(\mu^+\mu^- \to \tilde{\chi}_1^+\tilde{\chi}_1^-) \;=\; \frac{\sqrt{\lambda_{11}}}{8\pi s^2}\bar{P}, \tag{61}$$

and the charge asymmetry $\mathcal{A}_\lambda^C$ (47)

$$\Sigma_r^{3(HA)} = \frac{16\pi s^2}{\eta_{\lambda^+}\sqrt{\lambda_{11}}}\,\sigma(\mu^+\mu^- \to \tilde{\chi}_1^+\tilde{\chi}_1^-)\,\mathcal{A}_\lambda^C. \tag{62}$$

Now the product of couplings κ can be determined by a comparison of (62) with (60). Alternatively, using the polarization asymmetry $\mathcal{A}_{\lambda^\pm}^{pol}$ (49), we find

$$\Sigma_r^{3(HA)} = \frac{16\pi s^2}{\eta_{\lambda^\pm}\sqrt{\lambda_{11}}}\,\sigma(\mu^+\mu^- \to \tilde{\chi}_1^+\tilde{\chi}_1^-)\,\mathcal{A}_{\lambda^\pm}^{pol}. \tag{63}$$

In addition, a measurement of the asymmetries $\mathcal{A}_\lambda^C$ (47) or $\mathcal{A}_{\lambda^\pm}^{pol}$ (49) allows the determination of the ratio

$$\frac{\Sigma_r^3}{P_r} \;=\; \frac{\sigma(\mu^+\mu^- \to \tilde{\chi}_1^+\tilde{\chi}_1^-)}{\sigma_r(\mu^+\mu^- \to \tilde{\chi}_1^+\tilde{\chi}_1^-)}\frac{2}{\eta_{\lambda^+}}\mathcal{A}_\lambda^C \tag{64}$$

$$\;=\; \frac{\sigma(\mu^+\mu^- \to \tilde{\chi}_1^+\tilde{\chi}_1^-)}{\sigma_r(\mu^+\mu^- \to \tilde{\chi}_1^+\tilde{\chi}_1^-)}\frac{2}{\eta_{\lambda^\pm}}\mathcal{A}_{\lambda^\pm}^{pol}, \tag{65}$$

using the charge or polarization asymmetry, respectively. The resonant contributions

$$\sigma_r(\mu^+\mu^- \to \tilde{\chi}_1^+\tilde{\chi}_1^-) \;=\; \frac{\sqrt{\lambda_{11}}}{8\pi s^2}P_r, \quad \text{with} \quad P_r = \bar{P}_r, \tag{66}$$

to the cross section can be obtained by subtracting the continuum contributions. The latter can be estimated by extrapolating the production line shape below and above the resonance region [9]. Uncertainties due to detection efficiencies of the chargino decay products cancel out in the ratio

$$\frac{\sigma_r(\mu^+\mu^- \to \tilde{\chi}_1^+\chi_1^-)}{\sigma(\mu^+\mu^- \to \tilde{\chi}_1^+\chi_1^-)} \quad = \quad \frac{P_r}{\bar{P}}. \tag{67}$$

After inserting the expressions of $\Sigma_r^{3(HA)}$ (60) and P_r (24) we obtain

$$\frac{\Sigma_r^3}{P_r} \quad = \quad \frac{2\mathcal{P}}{1+\mathcal{P}^2}\,\frac{2\gamma\,\mathrm{Re}\{\Delta(H)\Delta^*(A)\}\sqrt{s^+ s}}{r\,|\Delta(H)|^2\,s^+ + r^{-1}\,|\Delta(A)|^2\,s}, \tag{68}$$

with

$$s^+ \quad = \quad s - 4m_{\chi_1^\pm}^2 = \frac{\lambda_{11}}{s}, \tag{69}$$

$$r \quad = \quad \frac{|c^{(H\mu)}c_R^{(H)}|}{|c^{(A\mu)}c_R^{(A)}|}. \tag{70}$$

It is now possible to solve (68) for r as well as for γ.

For our analysis we have assumed that the masses and widths of the Higgs resonances H and A can be measured. The resonance parameters of nearly degenerate Higgs bosons with different CP quantum numbers may e.g. be determined by using transverse beam polarizations, which enhances or suppresses the Higgs exchange channels depending on their CP quantum numbers [13].

Note that γ (59) can only be determined by measuring the charge or polarization asymmetries $\mathcal{A}_\lambda^C$ and $\mathcal{A}_{\lambda^\pm}^{pol}$, which are sensitive to the H–A interference channels. A determination of γ from a measurement of the cross section $\sigma(\mu^+\mu^- \to \tilde{\chi}_1^+\tilde{\chi}_1^-)$ is not possible, since it contains contributions from pure H or A exchange only.

4 Numerical results

We analyze numerically the charge asymmetry $\mathcal{A}_\ell^C$ (46) of the lepton energy distribution for the production of equal charginos $\mu^+\mu^- \to \tilde{\chi}_1^+\tilde{\chi}_1^-$ in Section 4.1, and the cross section asymmetry $\mathcal{A}_{prod}^C$ (54) for the production of different charginos in Section 4.2. The feasibility of measuring the asymmetries depends also on the corresponding production cross sections which we discuss in our scenarios. For the calculation of the Higgs masses and widths we use the program HDECAY [14]. For the calculation of the branching ratios and widths of the decaying charginos we include the two-body decays

$$\tilde{\chi}_1^\pm \quad \to \quad e^\pm\tilde{\nu}_e,\ \mu^\pm\tilde{\nu}_\mu,\ \tau^\pm\tilde{\nu}_\tau,\ \tilde{e}_L^\pm\nu_e,\ \tilde{\mu}_L^\pm\nu_\mu,\ \tilde{\tau}_{1,2}^\pm\nu_\tau,\ W^\pm\tilde{\chi}_n^0, \tag{71}$$

and neglect three-body decays. In order to reduce the number of parameters, we assume GUT relations for the gaugino mass parameters, related by $M_1 =$

$5/3\, M_2 \tan^2\theta_W$, and for the slepton masses, related to the scalar mass parameter m_0 at the GUT scale by the approximate renormalization group equations [15]

$$m^2_{\tilde{\ell}_R} = m_0^2 + 0.23 M_2^2 - m_Z^2 \cos 2\beta \sin^2\theta_W, \quad (72)$$

$$m^2_{\tilde{\ell}_L} = m_0^2 + 0.79 M_2^2 + m_Z^2 \cos 2\beta (-\frac{1}{2} + \sin^2\theta_W), \quad (73)$$

$$m^2_{\tilde{\nu}_\ell} = m_0^2 + 0.79 M_2^2 + \frac{1}{2} m_Z^2 \cos 2\beta. \quad (74)$$

In the stau sector we fix the trilinear scalar coupling parameter $A_\tau = 250$ GeV.

4.1 Production of $\tilde{\chi}_1^+ \tilde{\chi}_1^-$

In the following subsections we study the dependence of the asymmetries and cross sections on the MSSM parameters μ, M_2, $\tan\beta$ and m_A, as well as on the center of mass energy $\sqrt{s}$.

4.1.1 μ and M_2 dependence

In Fig. 2a we show the contour lines of the chargino production cross section $\sigma(\mu^+\mu^- \to \tilde{\chi}_1^+ \tilde{\chi}_1^-)$ in the μ–M_2 plane for $\sqrt{s} = m_A$ and beam polarizations $\mathcal{P}_+ = \mathcal{P}_- = -0.3$, with $m_A = 500$ GeV, $\tan\beta = 10$ and $m_0 = 70$ GeV. At $\sqrt{s} = m_A \approx m_H$ the production cross section is close to its peak value, since the two Higgs resonances are nearly degenerate. The main contributions to the cross section, which reaches up to 2 pb, are from the resonant ones. For increasing values of $|\mu|$ the couplings of both H and A to the charginos decrease, leading to smaller resonant contributions. The continuum contributions from γ, Z and $\tilde{\nu}_\mu$ exchange reach 0.5 pb at most.

We show contour lines of the chargino branching ratio $\mathrm{BR}(\tilde{\chi}_1^+ \to e^+ \tilde{\nu}_e)$ in the μ–M_2 plane in Fig. 2b, where also the allowed region for the chargino two-body decay $\tilde{\chi}_1^+ \to e^+ \tilde{\nu}_e$ is indicated. The sneutrinos are rather light for $m_0 = 70$ GeV, such that this chargino decay mode is open for $|\mu| \gtrsim 200$ GeV and reaches values of up to 20%.

For the chargino decay into an electron $\tilde{\chi}_1^\pm \to e^\pm \tilde{\nu}_e^{(*)}$, we show in Fig. 2c contour lines of the charge asymmetry $\mathcal{A}_e^C$ (46) which reaches values of up to 24%. The asymmetry depends only weakly on the character of chargino mixing, since $\mathcal{A}_e^C$ is proportional to a ratio of the couplings, see (64) and (68). In the ideal case of maximal H-A interference and vanishing continuum contributions, the asymmetry could reach its maximum absolute value of $|\mathcal{P}_+ + \mathcal{P}_-|/(1 + \mathcal{P}_+\mathcal{P}_-)/2 \approx 28\%$, as follows from (47) for $\mathcal{P}_+ = \mathcal{P}_- = -0.3$. Thus the shown values of $\mathcal{A}_e^C$ in Fig. 2c are large, since the amplitudes of the interfering H and A Higgs bosons are roughly of the same magnitude in the resonance region $\sqrt{s} = m_A$. Near the production threshold $\sqrt{s} = 2m_{\chi_1^\pm}$ the asymmetry decreases due to the p-wave suppression of the CP even scalar exchange amplitude.

In Fig. 2d we show the contour lines of the significance $\mathcal{S}_e^C$ (56) for an integrated effective luminosity $\mathcal{L}_{eff} = 1\ \mathrm{fb}^{-1}$. Due to the large asymmetry $\mathcal{A}_e^C$ and cross section $\sigma(\mu^+\mu^- \to \tilde{\chi}_1^+ \tilde{\chi}_1^-) \times \mathrm{BR}(\tilde{\chi}_1^+ \to e^+ \tilde{\nu}_e)$ for chargino production and subsequent decay,

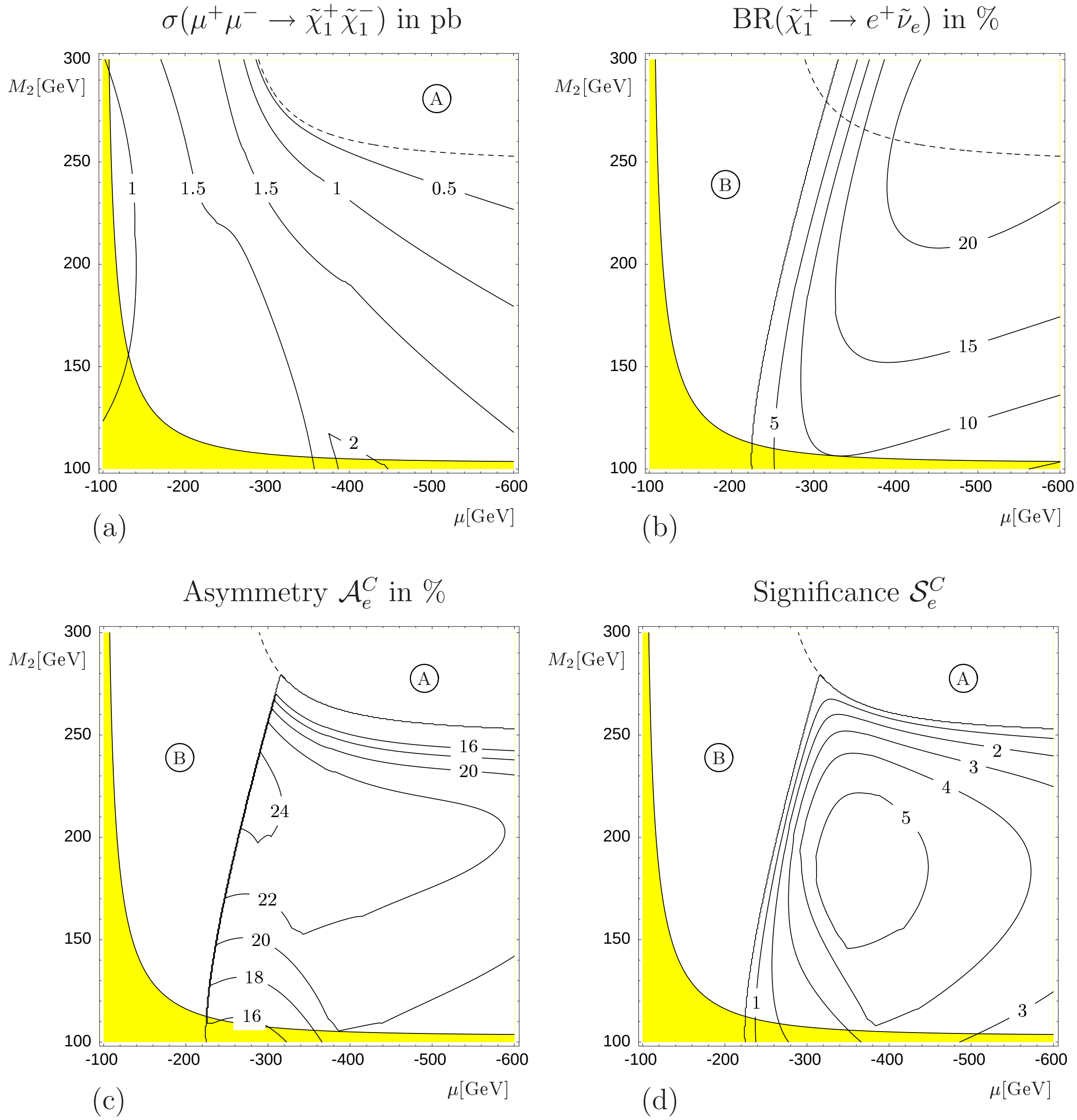

Figure 2: $\mu^+\mu^- \to \tilde{\chi}_1^+\tilde{\chi}_1^-$, $\tilde{\chi}_1^+ \to e^+\tilde{\nu}_e$. Contour lines of the cross section $\sigma(\mu^+\mu^- \to \tilde{\chi}_1^+\tilde{\chi}_1^-)$ **(a)**, the branching ratio BR($\tilde{\chi}_1^+ \to e^+\tilde{\nu}_e$) **(b)**, the charge asymmetry $\mathcal{A}_e^C$ **(c)** and the significance $\mathcal{S}_e^C$ for $\mathcal{L}_{eff} = 1\ \mathrm{fb}^{-1}$ **(d)** in the μ–M_2 plane for $m_A = 500$ GeV, $\tan\beta = 10$, $m_0 = 70$ GeV, $\sqrt{s} = 500$ GeV and longitudinal beam polarizations $\mathcal{P}_+ = \mathcal{P}_- = -0.3$. The dashed line indicates the kinematical limit $2m_{\chi_1^\pm} = \sqrt{s}$. The area A (B) is kinematically forbidden by $2m_{\chi_1^\pm} > \sqrt{s}$ ($m_{\tilde{\nu}_e} > m_{\chi_1^\pm}$). The shaded area is excluded by $m_{\chi_1^\pm} < 103$ GeV.

$\mathcal{A}_e^C$ can be measured with a significance $\mathcal{S}_e^C > 1$ for a luminosity $\mathcal{L}_{eff} = \mathcal{O}(\mathrm{fb}^{-1})$. The same values of the significance are obtained for the muonic chargino decay mode $\tilde{\chi}_1^+ \to \mu^+\tilde{\nu}_\mu$.

Table 1: Scenario **A** for $\mu^+\mu^- \to \tilde{\chi}_1^+\tilde{\chi}_1^-$.

$\tan\beta = 10$	$m_A = 500$ GeV	$m_{\chi_1^\pm} = 197$ GeV	$\mathrm{BR}(\tilde{\chi}_1^+ \to e^+\tilde{\nu}_e) = 19\%$
$\mu = -500$ GeV	$\Gamma_A = 1.41$ GeV	$m_{\chi_2^\pm} = 514$ GeV	$\mathrm{BR}(\tilde{\chi}_1^+ \to \mu^+\tilde{\nu}_\mu) = 19\%$
$M_2 = 200$ GeV	$m_H = 500.07$ GeV	$m_{\chi_1^0} = 100$ GeV	$\mathrm{BR}(\tilde{\chi}_1^+ \to \tau^+\tilde{\nu}_\tau) = 19\%$
$m_0 = 70$ GeV	$\Gamma_H = 1.20$ GeV	$m_{\tilde{\nu}_e} = 180$ GeV	$\mathrm{BR}(\tilde{\chi}_1^+ \to \tilde{\tau}_1^+\nu_\tau) = 43\%$

Table 2: Scenario **B7** for $\mu^+\mu^- \to \tilde{\chi}_1^+\tilde{\chi}_1^-$, chargino and slepton parameters.

$\tan\beta = 7$	$m_{\chi_1^\pm} = 158$ GeV	$\mathrm{BR}(\tilde{\chi}_1^+ \to e^+\tilde{\nu}_e) = 22\%$
$\mu = -400$ GeV	$m_{\chi_2^\pm} = 417$ GeV	$\mathrm{BR}(\tilde{\chi}_1^+ \to \mu^+\tilde{\nu}_\mu) = 22\%$
$M_2 = 160$ GeV	$m_{\chi_1^0} = 81$ GeV	$\mathrm{BR}(\tilde{\chi}_1^+ \to \tau^+\tilde{\nu}_\tau) = 22\%$
$m_0 = 70$ GeV	$m_{\tilde{\nu}_e} = 145$ GeV	$\mathrm{BR}(\tilde{\chi}_1^+ \to \tilde{\tau}_1^+\nu_\tau) = 33\%$

4.1.2 $\sqrt{s}$ dependence

In order to study the dependence of the asymmetries and the chargino production cross sections on the center of mass energy, we choose a representative point in the μ–M_2 plane with $\mu = -500$ GeV and $M_2 = 200$ GeV. The parameters and resulting Higgs masses and widths for this point, called scenario **A**, are given in Table 1. For the calculation of the branching ratios we include mixing in the stau sector, see e.g. [1, 16]. Note that $\mathrm{BR}(\tilde{\chi}_1^+ \to W^+\tilde{\chi}_1^0) < 0.3\%$ due to the small $\tilde{\chi}_1^+$-W^+-$\tilde{\chi}_1^0$ coupling in the gaugino scenario **A**, and $\mathrm{BR}(\tilde{\chi}_1^+ \to \tilde{e}_L^+\nu_e) < 0.01\%$ due to kinematical reasons since $m_{\chi_1^\pm} \approx m_{\tilde{e}_L}$.

In Fig. 3a we show the energy distribution asymmetry $\mathcal{A}_{e^+}$ (44) for the decay $\tilde{\chi}_1^+ \to e^+\tilde{\nu}_e$, and the asymmetry $\mathcal{A}_{e^-}$ for the charge conjugated process, with longitudinal beam polarizations $\mathcal{P}_+ = \mathcal{P}_- = -0.3$. In addition we show the charge asymmetry $\mathcal{A}_e^C = (\mathcal{A}_{e^+} - \mathcal{A}_{e^-})/2$, see (46), which reaches its maximal value of 23% at $\sqrt{s} \approx m_A = 500$ GeV. Since the continuum contributions from γ, Z and $\tilde{\nu}_\mu$ exchange cancel out, $\mathcal{A}_e^C$ asymptotically vanishes far from the resonance region. The $\sqrt{s}$ dependence of the chargino production cross section is shown in Fig. 3b. We show the corresponding statistical significance $\mathcal{S}_e^C$, defined in (56), for an effective integrated luminosity $\mathcal{L}_{eff} = 1\ \mathrm{fb}^{-1}$ in Fig. 3c.

4.1.3 m_A and $\tan\beta$ dependence

In Fig. 4a we compare the charge asymmetries $\mathcal{A}_e^C$ (46) for scenarios **B7**, **B7'** and **B7"**, that differ only in $m_A = \{350, 400, 500\}$ GeV, as a function of $\sqrt{s} - m_A$. We show the corresponding cross sections for $\mu^+\mu^- \to \tilde{\chi}_1^+\tilde{\chi}_1^-$ in Fig. 4b. For increasing Higgs masses their widths increase, and thus the interference of the H and A exchange amplitudes. However, the maxima of the asymmetries are reduced by

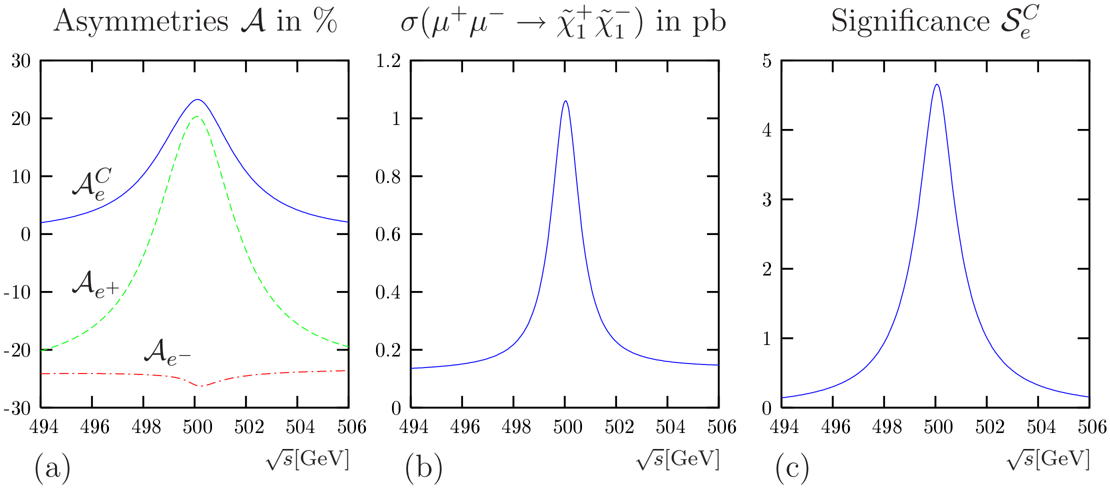

Figure 3: $\mu^+\mu^- \to \tilde{\chi}_1^+\tilde{\chi}_1^-$, $\tilde{\chi}_1^\pm \to e^\pm\tilde{\nu}_e^{(*)}$. Asymmetries **(a)**, chargino production cross section **(b)** and significance for $\mathcal{L}_{eff} = 1$ fb^{-1} **(c)**, with longitudinal beam polarizations $\mathcal{P}_+ = \mathcal{P}_- = -0.3$ for Scenario **A**, given in Table 1.

Table 3: Scenarios **B7**, **B7'** and **B7"**, Higgs sector parameters.

	B7	**B7'**	**B7"**
m_A[GeV]	350	400	500
m_H[GeV]	350.7	400.6	500.4
Γ_A[GeV]	0.56	1.00	1.4
Γ_H[GeV]	0.43	0.65	1.1

larger continuum contributions to the cross section. For smaller Higgs masses, here $m_A = 350$ GeV, the threshold effects are stronger. Since a Dirac fermion-antifermion pair has negative intrinsic parity, and thus the CP even H resonance is p-wave suppressed, the peak cross section is found at $\sqrt{s} \approx m_A$, where the asymmetry nearly vanishes. The asymmetry changes sign between the two resonances, whose mass difference is larger than their widths, due to the complex phases of the propagators. Its maximum is found at center of mass energies slightly above m_H where the phases of the propagators are roughly equal and the amplitudes of similar magnitude. In Fig. 4c we show the statistical significance $\mathcal{S}_e^C$ for an integrated effective luminosity $\mathcal{L}_{eff} = 1$ fb^{-1}. We find statistical significances of $\mathcal{S}_e^C > 3$, albeit not in the entire resonance region for scenarios **B7** and **B7'** with smaller m_A.

The asymmetries are also sensitive to a variation of $\tan\beta$. In the Higgs sector, increasing $\tan\beta$ results in larger H and A widths and smaller mass differences between H and A. This leads to a larger overlap of the two resonances, and thus to larger asymmetries $\mathcal{A}_e^C$ in the resonance region. In addition, since the couplings of the muons to the Higgs bosons (6) and (7) are proportional to $\tan\beta$ in the Higgs decoupling limit [17], larger values of $\tan\beta$ imply smaller relative continuum con-

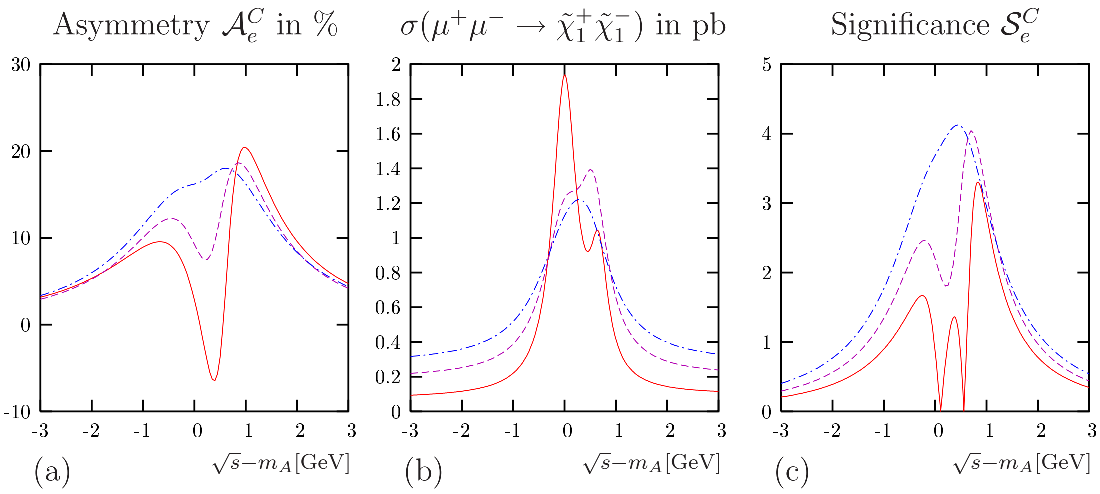

Figure 4: $\mu^+\mu^- \to \tilde{\chi}_1^+\tilde{\chi}_1^-$, $\tilde{\chi}_1^\pm \to e^\pm\tilde{\nu}_e^{(*)}$. Asymmetry $\mathcal{A}_e^C$ **(a)**, cross section $\sigma(\mu^+\mu^- \to \tilde{\chi}_1^+\tilde{\chi}_1^-)$ **(b)** and significance $\mathcal{S}_e^C$ for $\mathcal{L}_{eff} = 1$ fb^{-1} **(c)** for scenarios **B7** (solid), **B7'** (dashed) and **B7"** (dot-dashed) of Tables 2 and 3 with $m_A = 350$ GeV, 400 GeV and 500 GeV, respectively, and longitudinal beam polarizations $\mathcal{P}_+ = \mathcal{P}_- = -0.3$.

tributions that enhance the asymmetries. On the contrary, for small $\tan\beta \lesssim 5$ and $m_{H,A} < 2m_t$, with m_t the top quark mass, the resonances practically do not overlap, see e.g. [9], and the asymmetries cannot be measured. For $m_{H,A} > 2m_t$, the resulting large H and A widths may lead to an overlap of the resonances. However, the combined effect of smaller Higgs-muon couplings and the suppression of the cross section due to the large widths imply a small resonant contribution with respect to the continuum and consequently only small asymmetries and statistical significances are obtained.

4.1.4 Chargino decay into a W boson

If the sleptons are heavier than the charginos, the chargino decay into a W boson, $\tilde{\chi}_1^\pm \to W^\pm\tilde{\chi}_1^0$, might be the only allowed two-body decay channel. In this case only the asymmetries of the energy distribution of the W boson, $\mathcal{A}_W^C$ (46) and $\mathcal{A}_{W^\pm}^{pol}$ (48) are accessible. These asymmetries are reduced by a factor $\eta_{W^\pm}$ (B.15) with respect to the asymmetries for leptonic chargino decay modes. In Fig. 2c we have shown the contour lines of the leptonic charge asymmetry $\mathcal{A}_e^C$ (46) in the μ–M_2 plane for $\tan\beta = 10$. The values of $\mathcal{A}_e^C$ have to be multiplied by $\eta_{W^+} = -\eta_{W^-}$, which we show in Fig. 5, to obtain the asymmetry $\mathcal{A}_W^C = \eta_{W^+} \times \mathcal{A}_e^C$. Although the asymmetries are suppressed by $|\eta_{W^\pm}| \approx 0.2 - 0.4$, and uncertainties in the energy measurement of the W boson lead to lower effective integrated luminosities, statistics will be gained from large branching ratios, $\mathrm{BR}(\tilde{\chi}_1^\pm \to W^\pm\tilde{\chi}_1^0) = 1$.

4.2 Production of $\tilde{\chi}_1^\pm\tilde{\chi}_2^\mp$

In Fig. 6a we show the cross sections for $\mu^+\mu^- \to \tilde{\chi}_1^+\tilde{\chi}_2^-$ production and for the charge conjugated process $\mu^+\mu^- \to \tilde{\chi}_1^-\tilde{\chi}_2^+$ for scenario **P1**, given in Table 4. The

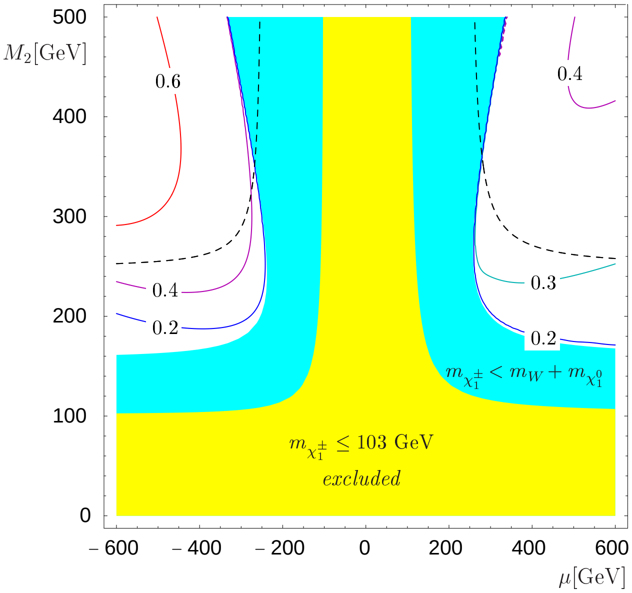

Figure 5: Contour lines of η_{W^-} (B.15) for the decay $\tilde{\chi}_1^- \to W^- \tilde{\chi}_1^0$ in the μ–M_2 plane for $\tan\beta = 10$. The dashed line indicates the kinematical limit for $2m_{\chi_1^\pm} = \sqrt{s} = 500$ GeV. The dark shaded area is kinematically forbidden by $m_{\chi^\pm} < m_W + m_{\chi_1^0}$. The light shaded area is experimentally excluded by $m_{\chi_1^\pm} < 103$ GeV.

Table 4: Scenarios **P1** and **P2** for $\mu^+\mu^- \to \tilde{\chi}_1^\pm \tilde{\chi}_2^\mp$.

	P1	**P2**		**P1**	**P2**
$\tan\beta$	10	10	$m_{\chi_1^\pm}$[GeV]	138	106
μ[GeV]	−250	−110	$m_{\chi_2^\pm}$[GeV]	281	322
M_2[GeV]	150	300	$m_{\chi_1^0}$[GeV]	74	89
m_0[GeV]	200	200	$m_{\tilde{\nu}_\mu}$[GeV]	232	327
m_A[GeV]	500	500	Γ_A[GeV]	3.7	3.4
m_H[GeV]	500.3	500.4	Γ_H[GeV]	3.6	3.3

two cross sections are equal for unpolarized beams and differ for polarized beams $\mathcal{P}_+ = \mathcal{P}_- = -0.3$. In this case the H–A interference (25) enhances the $\tilde{\chi}_1^- \tilde{\chi}_2^+$ cross section and suppresses that for the conjugated process. The corresponding asymmetry $\mathcal{A}_{prod}^C$ (54) of the two cross sections is $\mathcal{A}_{prod}^C = -48\%$ at $\sqrt{s} = 500$ GeV. The asymmetry almost reaches its maximum absolute value of $|\mathcal{P}_+ + \mathcal{P}_-|/(1 + \mathcal{P}_+\mathcal{P}_-) \approx 55\%$, here for $\mathcal{P}_+ = \mathcal{P}_- = -0.3$, which would be obtained in the ideal case of vanishing continuum contributions. For scenario **P2**, shown in Fig. 6b, the $\tilde{\chi}_1^- \tilde{\chi}_2^+$ production is instead suppressed by the H–A interference and the $\tilde{\chi}_1^+ \tilde{\chi}_2^-$ production is enhanced, such that $\mathcal{A}_{prod}^C = 45\%$ changes sign. In scenario **P1** (**P2**) the lightest chargino has mainly gaugino (higgsino) character, i.e., the gaugino (higgsino) components

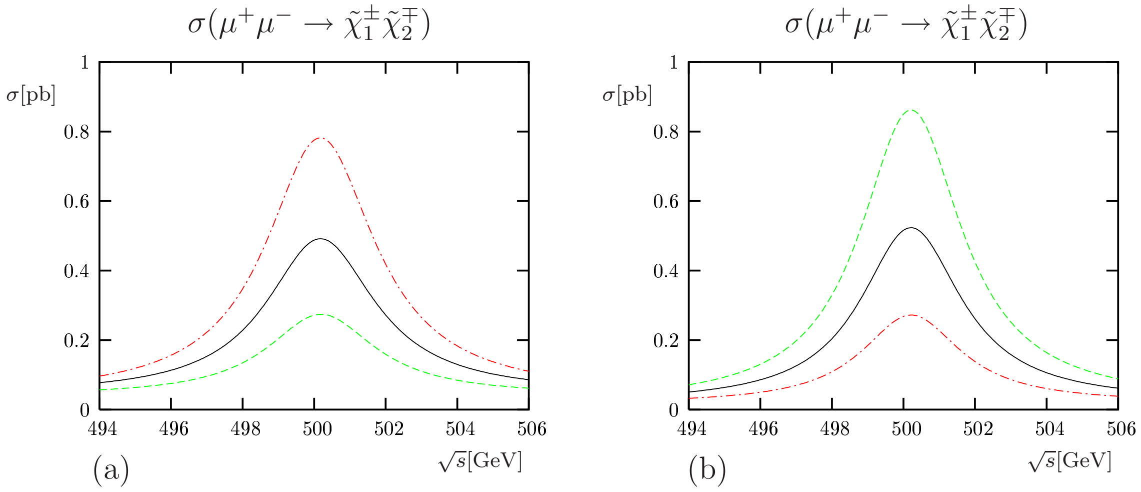

Figure 6: $\mu^+\mu^- \to \tilde{\chi}_1^\pm \tilde{\chi}_2^\mp$. Cross sections $\sigma(\mu^+\mu^- \to \tilde{\chi}_1^+ \tilde{\chi}_2^-)$ (dashed) and $\sigma(\mu^+\mu^- \to \tilde{\chi}_1^- \tilde{\chi}_2^+)$ (dash-dotted) for longitudinal beam polarizations $\mathcal{P}_+ = \mathcal{P}_- = \mathcal{P} = -0.3$, and $\sigma(\mu^+\mu^- \to \tilde{\chi}_1^\pm \tilde{\chi}_2^\mp)$ (solid) for $\mathcal{P} = 0$, for scenario **P1 (a)** and scenario **P2 (b)**, given in Table 4.

are larger. Since Higgs bosons couple to a gaugino-higgsino pair, the corresponding couplings (8-10) transform as $c_{L,R\,ij}^{(\phi)} \leftrightarrow c_{L,R\,ji}^{(\phi)}$ under $M_2 \leftrightarrow |\mu|$. This transformation relates the resonant amplitudes of $\tilde{\chi}_1^+ \tilde{\chi}_2^-$ and $\tilde{\chi}_1^- \tilde{\chi}_2^+$ production for scenarios **P1** and **P2**, which explains the different signs of $\mathcal{A}_{prod}^C$. Consequently for $M_2 = |\mu|$ the asymmetries vanish, even for polarized beams.

5 Summary and conclusions

In the CP conserving MSSM we have studied the s-channel interference of the CP even and CP odd neutral Higgs bosons H and A in chargino production $\mu^+\mu^- \to \tilde{\chi}_i^\mp \tilde{\chi}_j^\pm$ with longitudinally polarized beams. We have shown that the interference of H and A can be analyzed for $\tilde{\chi}_1^+ \tilde{\chi}_1^-$ production using asymmetries in the energy distribution of the lepton or W boson from the decay $\tilde{\chi}_1^\pm \to \ell^\pm \tilde{\nu}_\ell$, $\ell = e, \mu, \tau$, or $\tilde{\chi}_1^\pm \to W^\pm \tilde{\chi}_1^0$, respectively. The asymmetries of the energy distributions are correlated to the longitudinal chargino polarizations. For the production of two different charginos, the H–A interference can be analyzed using asymmetries of the $\tilde{\chi}_1^+ \tilde{\chi}_2^-$ cross section and its charge conjugate. The asymmetries depend on the muon beam polarizations and thus vanish for unpolarized beams. Since the asymmetries probe the H–A interference, their measurement allows a determination of chargino couplings to the H and A bosons as well as a determination of the relative phase of the couplings. In a numerical study we have analyzed the production of $\tilde{\chi}_1^+ \tilde{\chi}_1^-$ and $\tilde{\chi}_1^\pm \tilde{\chi}_2^\mp$ for different MSSM scenarios and found asymmetries which are maximal for nearly degenerate H and A bosons. In the numerical analysis of the chargino cross sections and branching ratios, we have shown that the asymmetries are accessible at a future muon collider with polarized beams.

Appendix

A Chargino polarization vectors

We choose a coordinate frame in the center of mass system (CMS) such that the momentum of the chargino $\tilde{\chi}_j^{\pm}$ is given by

$$p^{\mu}_{\chi_j^{\pm}} = (E_{\chi_j^{\pm}}; 0, 0, |\vec{p}_{\chi_j^{\pm}}|), \tag{A.1}$$

with

$$E_{\chi_j^{\pm}} = \frac{s + m^2_{\chi_j^{\pm}} - m^2_{\chi_i^{\pm}}}{2\sqrt{s}}, \quad |\vec{p}_{\chi_j^{\pm}}| = \frac{\lambda^{\frac{1}{2}}(s, m^2_{\chi_i^{\pm}}, m^2_{\chi_j^{\pm}})}{2\sqrt{s}}. \tag{A.2}$$

The spin vectors of the chargino are then defined by

$$s^{1,\mu}_{\chi_j^{\pm}} = (0; 1, 0, 0), \qquad s^{2,\mu}_{\chi_j^{\pm}} = (0; 0, 1, 0), \qquad s^{3,\mu}_{\chi_j^{\pm}} = \frac{1}{m_{\chi_j^{\pm}}}(|\vec{p}_{\chi_j^{\pm}}|; 0, 0, E_{\chi_j^{\pm}}). \tag{A.3}$$

B Chargino decay into τ and W boson

The interaction Lagrangians for chargino decay into a τ, $\tilde{\chi}_j^{\pm} \to \tau^{\pm}\ \tilde{\nu}_{\tau}^{(*)}$, and W boson, $\tilde{\chi}_j^{\pm} \to W^{\pm}\ \tilde{\chi}_k^0$, are, respectively [1]

$$\begin{aligned} \mathcal{L}_{\tau\tilde{\nu}_{\tau}\tilde{\chi}^+} &= -g\bar{\tau}(V_{j1}P_R - Y_{\tau}U^*_{j2}P_L)\tilde{\chi}_j^{+C}\tilde{\nu}_{\tau} + \text{h.c.}, && \text{(B.4)} \\ \mathcal{L}_{W^-\tilde{\chi}^+\tilde{\chi}^0} &= gW^-_{\mu}\bar{\tilde{\chi}}^0_k\gamma^{\mu}(O^L_{kj}P_L + O^R_{kj}P_R)\tilde{\chi}_j^{+}\tilde{\nu}_{\ell} + \text{h.c.}, && \text{(B.5)} \end{aligned}$$

with the couplings

$$\begin{aligned} O^L_{kj} &= -\frac{1}{\sqrt{2}}N_{k4}V^*_{j2} + (\sin\theta_W N_{k1} + \cos\theta_W N_{k2})V^*_{j1}, && \text{(B.6)} \\ O^R_{kj} &= +\frac{1}{\sqrt{2}}N^*_{k3}U_{j2} + (\sin\theta_W N^*_{k1} + \cos\theta_W N^*_{k2})U_{j1}, && \text{(B.7)} \end{aligned}$$

and $Y_{\tau} = m_{\tau}/(\sqrt{2}m_W\cos\beta)$. The 4×4 unitary matrix N diagonalizes the neutralino mass matrix Y in the basis $\{\tilde{\gamma}, \tilde{Z}, \tilde{h}_1, \tilde{h}_2\}$ with $N^*_{il}Y_{lm}N^{\dagger}_{mj} = \delta_{ij}m_{\chi^0_j}$ [1].

The expansion coefficients of the chargino decay matrix (18) for $\tilde{\chi}_j^{+} \to \tau^{+}\ \tilde{\nu}_{\tau}$ are

$$\begin{aligned} D &= \frac{g^2}{2}(|V_{j1}|^2 + Y_{\tau}^2|U_{j2}|^2)(m^2_{\chi_j^{\pm}} - m^2_{\tilde{\nu}_{\tau}}), && \text{(B.8)} \\ \Sigma^a_D &= -g^2(|V_{j1}|^2 - Y_{\tau}^2|U_{j2}|^2)m_{\chi_j^{\pm}}(s^a_{\chi_j^{\pm}}\cdot p_{\tau}), && \text{(B.9)} \end{aligned}$$

and those for $\tilde{\chi}_j^{+} \to W^{+}\ \tilde{\chi}_k^0$ are

$$\begin{aligned} D &= \frac{g^2}{2}(|O^L_{kj}|^2 + |O^R_{kj}|^2)\left[m^2_{\chi_j^{\pm}} + m^2_{\chi_k^0} - 2m_W^2 + \frac{(m^2_{\chi_j^{\pm}} - m^2_{\chi_k^0})^2}{m_W^2}\right] \\ &\quad -6g^2\text{Re}(O^L_{kj}O^{R*}_{kj})m_{\chi_j^{\pm}}m_{\chi_k^0}, && \text{(B.10)} \\ \Sigma^a_D &= -g^2(|O^L_{kj}|^2 - |O^R_{kj}|^2)\frac{(m^2_{\chi_j^{\pm}} - m^2_{\chi_k^0} - 2m_W^2)}{m_W^2}m_{\chi_j^{\pm}}(s^a_{\chi_j^{\pm}}\cdot p_W). && \text{(B.11)} \end{aligned}$$

The coefficients Σ_D^a for the charge conjugated processes, $\tilde{\chi}_j^- \to \tau^- \ \tilde{\nu}_\tau^*$ and $\tilde{\chi}_j^- \to W^- \ \tilde{\chi}_k^0$, are obtained by inverting the signs of (B.9) and (B.11), respectively.

For the chargino decay $\tilde{\chi}_j^\pm \to W^\pm \ \tilde{\chi}_k^0$ the energy limits of the W boson are $E_W^{max(min)} = \bar{E}_W \pm \Delta_W$, see (37), with

$$\bar{E}_W = \frac{E_W^{max} + E_W^{min}}{2} = \frac{m_{\chi_j^\pm}^2 + m_W^2 - m_{\chi_k^0}^2}{2m_{\chi_j^\pm}^2} E_{\chi_j^\pm}, \tag{B.12}$$

$$\Delta_W = \frac{E_W^{max} - E_W^{min}}{2} = \frac{\sqrt{\lambda(m_{\chi_j^\pm}^2, m_W^2, m_{\chi_k^0}^2)}}{2m_{\chi_j^\pm}^2} |\vec{p}_{\chi_j^\pm}|. \tag{B.13}$$

The factor $\eta_{\lambda^\pm}$ (40) for the decay $\tilde{\chi}_j^\pm \to \tau^\pm \ \tilde{\nu}_\tau^{(*)}$ is given by

$$\eta_{\tau^\pm} = \pm \frac{|V_{j1}|^2 - Y_\tau^2 |U_{j2}|^2}{|V_{j1}|^2 + Y_\tau^2 |U_{j2}|^2}. \tag{B.14}$$

For the decay $\tilde{\chi}_j^\pm \to W^\pm \ \tilde{\chi}_k^0$ we find

$$\eta_{W^\pm} = \pm \frac{(|O_{kj}^L|^2 - |O_{kj}^R|^2) f_1}{(|O_{kj}^L|^2 + |O_{kj}^R|^2) f_2 + \mathrm{Re}\{O_{kj}^L O_{kj}^{R*}\} f_3}, \tag{B.15}$$

with

$$\begin{aligned} f_1 &= (m_{\chi_j^\pm}^2 - m_{\chi_k^0}^2 - 2m_W^2)\sqrt{\lambda(m_{\chi_j^\pm}^2, m_W^2, m_{\chi_k^0}^2)}, \\ f_2 &= (m_{\chi_j^\pm}^2 + m_{\chi_k^0}^2 - 2m_W^2)\ m_W^2 + (m_{\chi_j^\pm}^2 - m_{\chi_k^0}^2)^2, \\ f_3 &= -12\ m_{\chi_j^\pm}\ m_{\chi_k^0}\ m_W^2. \end{aligned}$$

The coefficients $\eta_{\tau^\pm}$ and $\eta_{W^\pm}$ depend on the τ and W couplings to the charginos, as well as on the chargino and neutralino masses, which could be measured at the international linear collider (ILC) with high precision [18, 19].

References

[1] H. Haber, K. Kane, Phys. Rep. **117** (1985) 75.

[2] J. Gunion, H. Haber, Nucl. Phys. **B 272** (1986) 1.

[3] A. Djouadi, arXiv:hep-ph/0503173.

[4] Proceedings of *Prospective Study of Muon Storage Rings at CERN*, Eds. B. Autin, A. Blondel, J. Ellis, CERN yellow report, CERN 99-02, ECFA 99-197, April 30 (1999);
C. Blöchinger et al., Higgs working group of the ECFA-CERN study on Neutrino Factory & Muon Storage Rings at CERN, *Physics Opportunities at $\mu^+\mu^-$ Higgs Factories* CERN-TH/2002-028, [arXiv:hep-ph/0202199];
A. Blondel *et al.*, "ECFA/CERN studies of a European neutrino factory complex," CERN-2004-002.

[5] V. Barger, M.S. Berger, J.F. Gunion, T. Han, Nucl. Phys. Proc. Suppl. **51A** (1996) 13, [arXiv:hep-ph/9604334];
R. Casalbuoni et al., JHEP **9908** (1999) 011, [arXiv:hep-ph/9904268];
V. Barger, M.S. Berger, J.F. Gunion, T. Han, in *Proc. of the APS/DPF/DPB Summer Study on The Future of Particle Physics (Snowmass 2001)*, ed. R. Davidson and C. Quigg, [arXiv:hep-ph/0110340].

[6] V. Barger, M.S. Berger, J.F. Gunion, T. Han, Phys. Rep. **286** (1997) 1, [arXiv:hep-ph/9602415].

[7] E. Asakawa, A. Sugamoto and I. Watanabe, Eur. Phys. J. **C17** (2000) 279 [arXiv:hep-ph/0004005];
E. Asakawa, S. Y. Choi and J. S. Lee, Phys. Rev. D **63**, 015012 (2001) [arXiv:hep-ph/0005118].

[8] H. Fraas, F. von der Pahlen and C. Sachse, Eur. Phys. J. **C37** (2004) 495 [arXiv:hep-ph/0407057].

[9] H. Fraas, F. Franke, G. Moortgat-Pick, F. von der Pahlen and A. Wagner, Eur. Phys. J. C **29** (2003) 587 [arXiv:hep-ph/0303044].

[10] H. E. Haber, Proceedings of the 21st SLAC Summer Institute on Particle Physics: Spin Structure in High Energy Processes, SLAC, Stanford, CA 1993 [arXiv:hep-ph/9405376].

[11] G. Moortgat-Pick, H. Fraas, A. Bartl and W. Majerotto, Eur. Phys. J. C **7** (1999) 113 [arXiv:hep-ph/9804306].

[12] O. Kittel, arXiv:hep-ph/0504183.

[13] D. Atwood and A. Soni, Phys. Rev. D **52** (1995) 6271 [arXiv:hep-ph/9505233];
B. Grzadkowski and J. F. Gunion, Phys. Lett. B **350** (1995) 218 [arXiv:hep-ph/9501339];
J. F. Gunion, B. Grzadkowski and X. G. He, Phys. Rev. Lett. **77** (1996) 5172 [arXiv:hep-ph/9605326];
J. F. Gunion and J. Pliszka, Phys. Lett. B **444** (1998) 136 [arXiv:hep-ph/9809306];
B. Grzadkowski and J. Pliszka, Phys. Rev. D **60** (1999) 115018 [arXiv:hep-ph/9907206].

[14] A. Djouadi, J. Kalinowski, M. Spira, Comput. Phys. Commun. **108** (1998) 56, [arXiv:hep-ph/9704448].

[15] L. J. Hall and J. Polchinski, Phys. Lett. B **152**, 335 (1985).

[16] A. Bartl, K. Hidaka, T. Kernreiter and W. Porod, Phys. Rev. D **66** (2002) 115009 [arXiv:hep-ph/0207186].

[17] A. Dobado, M.J. Herrero and S. Penaranda, Eur. Phys. J. C **17** (2000) 487;
J.F. Gunion and H.E. Haber, Phys. Rev. D **67** (2003) 075019;
H.E. Haber and Y. Nir, Phys. Lett. B **306** (1993) 327;
H.E. Haber, CERN-TH/95-109 and arXiv:hep-ph/9505240.

[18] "TESLA Technical Design Report Part III: Physics at an e+e- Linear Collider," arXiv:hep-ph/0106315.

[19] M. M. Nojiri, Phys. Rev. D **51** (1995) 6281 [arXiv:hep-ph/9412374];
M. M. Nojiri, K. Fujii and T. Tsukamoto, Phys. Rev. D **54** (1996) 6756 [arXiv:hep-ph/9606370];
E. Boos, H. U. Martyn, G. Moortgat-Pick, M. Sachwitz, A. Sherstnev and P. M. Zerwas, Eur. Phys. J. C **30** (2003) 395 [arXiv:hep-ph/0303110];
A. Freitas, H. U. Martyn, U. Nauenberg and P. M. Zerwas, arXiv:hep-ph/0409129.